

## PROPERTIES OF SINGLE FAST CHLORIDE CHANNELS FROM RAT CEREBRAL CORTEX NEURONS

BY ANDREW L. BLATZ

*From the Department of Physiology, University of Texas Southwestern Medical Center, Dallas, TX 75235, USA*

*(Received 1 October 1990)*

### SUMMARY

1. Properties of  $\text{Cl}^-$  channels from surface membranes of acutely dissociated rat cerebral cortical neurons were studied with the patch clamp technique. These channels were present in the majority of excised inside-out membrane patches.

2.  $\text{Cl}^-$  channels were rarely observed in cell-attached membrane patches, and usually several minutes elapsed following excision of the patch before  $\text{Cl}^-$  channels became active.

3. Under asymmetric ionic conditions (1000 mM- $\text{KCl}_i$ , 140 mM- $\text{KCl}_o$ ), neuronal  $\text{Cl}^-$  channels are fairly selective for  $\text{Cl}^-$  over  $\text{K}^+$  and  $\text{Na}^+$ , with permeability ratios, determined by reversal potential shifts of 4.8 for both  $P_{\text{Cl}}/P_{\text{K}}$  and  $P_{\text{Cl}}/P_{\text{Na}}$ .

4. Neuronal  $\text{Cl}^-$  channel kinetic activity remained stable over periods of time long enough to collect up to 500 000 open and closed intervals. Occasionally, the channels entered altered modes of activity. In the 'buzz mode' the open and closed interval durations became much shorter than normal for several hundreds of intervals. In the 'subconductance mode' the channel opened to a current level about two-thirds of the normal level.

5. Using the method of maximum likelihood, sums of exponentials were fitted to the distributions of open and closed interval durations. Open interval distributions required at least two exponential components with time constants of  $< 1$  ms. At least six or seven exponential components were required to fit the closed interval distributions with time constants ranging from 30  $\mu\text{s}$  to several hundreds of milliseconds. This suggests that neuronal  $\text{Cl}^-$  channels enter at least two open and six or seven closed kinetic states during normal activity.

6.  $\text{Cl}^-$  channels often entered long-duration closed states of several minutes which could not be accounted for by the sums of exponentials fitted to the distribution of closed interval durations.

7. Neuronal  $\text{Cl}^-$  channels exhibit a marked voltage dependence with the percentage of time the channels are open increasing with depolarization. Most of the observed voltage dependence can be accounted for by a decrease in the mean closed interval duration with depolarization. The mean open interval was relatively independent of voltage.

8. These results suggest a high degree of similarity in kinetic behaviour and

conductance properties between the fast  $\text{Cl}^-$  channels of tissue-cultured rat skeletal muscle and fast  $\text{Cl}^-$  channels in acutely dissociated rat cerebral cortical neurons.

#### INTRODUCTION

Although  $\text{Cl}^-$ -selective ion channels activated by the neurotransmitters  $\gamma$ -aminobutyric acid (GABA) and glycine have been demonstrated in several mammalian neuronal cells (for review: Barker, Harrison & Owen, 1990), and their properties described in some detail,  $\text{Cl}^-$  channels that are not activated by these neurotransmitters have been described in only a few mammalian neuronal tissues, including tissue-cultured rat hippocampal neurons (Franciolini & Nonner, 1988; Franciolini & Petris, 1988) and tissue-cultured rat spinal cord neurons (Hughes, McBurney, Smith & Zorec, 1987). Non-transmitter activated  $\text{Cl}^-$ -selective channels ('background  $\text{Cl}^-$  channels', Franciolini & Petris, 1990) may play an important role in the nervous system by stabilizing the neuron resting membrane potential as they do in adult mammalian skeletal muscle (Bretag, 1987).

An important consideration regarding previous studies is that  $\text{Cl}^-$  channels were recorded in membranes from tissue-cultured embryonic-derived neuronal cells. Extrapolation of properties of channels found in these cells to those of fully differentiated, normally innervated mature neurons may be difficult especially in the light of evidence that the chloride conductances of embryonic and tissue-cultured mammalian skeletal muscle are quite different from those found in adult muscle (Bretag, 1987). Acute dissociation of cells from brains of postnatal animals avoids this potential problem.

The purpose of this study is to determine some of the properties of one type of  $\text{Cl}^-$  channel in acutely dissociated neurons of rat cerebral cortex. This channel shares many properties with the  $\text{Cl}^-$  channel recorded in tissue-cultured rat skeletal muscle ('fast  $\text{Cl}^-$  channel', Blatz & Magleby, 1983, 1986; Weiss & Magleby, 1990) and is somewhat similar to  $\text{Cl}^-$  channels recorded in tissue-cultured rat hippocampal neurons (Franciolini & Nonner, 1987; Franciolini & Petris, 1988). These channels are found in great abundance in dissociated neurons and may participate in a variety of neuronal functions.

A preliminary report of some of this work has been published (Blatz, 1990*c*).

#### METHODS

Single channel currents were recorded from dissociated rat cortical neurons using the inside-out configuration of the patch clamp technique (Hamill, Marty, Neher & Sakmann, 1981).

##### *Neuron dissociation*

Cortical neurons were obtained from young (4- to 15-day-old) Sprague-Dawley rats following the method of Kay & Wong (1986). Briefly, rats were killed by ether inhalation and their brains rapidly removed, sliced coronally at 0.5 mm, and immersed in ice-cold piperazine-*N,N'*-bis(2-ethanesulphonic acid) (PIPES)-buffered saline (see below for composition). Plugs of cortex approximately 0.5 mm in diameter were removed with an electrode blank and placed into PIPES saline containing 6 mg ml<sup>-1</sup> trypsin (Sigma type III) for 1 h at 37 °C. All solutions were continuously bubbled with 100% O<sub>2</sub>. The plugs were then washed three times and placed in PIPES-buffered saline at room temperature. When cells were needed, one or two of the plugs were

triturerated through a fire-polished pipette and the resultant suspension was placed into plastic tissue-culture dishes. Neurons were used within 6 h of being removed from the brain. A variety of cell morphologies was obtained with this method. All results in this study were obtained from large (12–17  $\mu\text{m}$  diameter), pyramidal-shaped neurons.

#### *Solutions*

During seal formation and initial excision, neurons were bathed externally in PIPES saline which contained (mM): 120 NaCl, 5 KCl, 1 CaCl<sub>2</sub>, 1 MgCl<sub>2</sub>, 25 glucose, 20 PIPES pH 7.0. The recording electrode (which bathed the extracellular membrane surface) contained (mM): 140 KCl, 5 TES (*N*-tris-hydroxymethyl-2-aminoethane sulphonic acid) buffer, 1 EGTA, 1.095 CaCl<sub>2</sub> ('free' Ca approximately 100  $\mu\text{M}$ ), titrated with KOH to pH 7.0. Unless otherwise indicated, the solution bathing the formerly intracellular membrane surface contained (mM): 1000 KCl, 5 TES, 1 EGTA, titrated with KOH to pH 7.0.

#### *Single-channel recording*

Single-channel currents were recorded with an Axopatch IIB patch clamp amplifier and stored on an FM tape-recorder with Bessel filtering characteristics (Racal Store 4DS) without additional filtering during experiments. For patches that contained a single active Cl<sup>-</sup> channel, data were recorded at the fastest tape speeds (30 or 60 in s<sup>-1</sup>; cut-off frequency of 16 or 32 kHz). When more than one channel was present in a patch, data were usually recorded at slower tape speeds (7.5 or 15 in s<sup>-1</sup>; cut-off frequency of 4 or 8 kHz).

The tip of the recording electrode containing the membrane patch was placed into a microchamber (Barrett, Magleby & Pallotta, 1982), where the bath solution could be rapidly and completely exchanged. Recordings were performed at room temperature (20–22 °C).

#### *Measuring open and closed interval durations*

Experimental data were played from the tape-recorder into a computer (DEC 11/73) at reduced tape speeds through a low-pass filter (Ithaco no. 4302, 24 dB octave<sup>-1</sup>, pulse (Bessel mode)), usually with an overall cut-off frequency of 6.2 kHz (–3 dB). Some data were analysed with lower cut-off frequencies when a lower signal-to-noise ratio required more filtering to reduce noise to an acceptable level. For dwell time analysis the effective sampling rate into the computer was 0.004 ms per point. Errors due to sampling promotion error are negligible at this rate (McManus, Blatz & Magleby, 1987). Open and closed intervals were measured as the times between threshold crossings at the 50% level with a machine language routine and the file of consecutive open and closed interval durations was stored on disc for later analysis.

Mean open and closed interval durations were calculated simply as the open or closed duration during a particular recording session divided by the number of open or closed events during that session. The percentage of time open was calculated as 100 times the total amount of time that the channel was in the open state divided by the total time of the record. In patches that contained a single active Cl<sup>-</sup> channel, the open probability ( $P_o$ ) is equal to the percentage of time open divided by 100.

The overall frequency response of the patch clamp amplifier, tape-recorder, and active filter is best described in terms of dead time. Intervals less than or equal to the dead time are not detected with a 50% threshold; all intervals with durations longer than the dead time are detected (Colquhoun & Sigworth, 1983). For example, for data analysed with the filter set at a cut-off frequency of 6.2 kHz, events less than about 0.03 ms are not detected, therefore, the dead time is 0.03 ms. Most of the data for the dwell time analysis were analysed with a dead time of 0.03 ms. Recordings that were filtered at lower cut-off frequencies were analysed with appropriately longer dead times.

#### *Fitting distributions of open and closed intervals*

Single-channel open and closed interval durations were measured and unconditional dwell time distributions analysed as described in detail previously (Blatz & Magleby, 1986, 1989; McManus, Blatz & Magleby, 1987). Briefly, detected open and closed interval durations were binned separately according to the logarithm of the interval duration (McManus, Blatz & Magleby, 1987). The distributions of open and closed interval durations were then fitted to the sums of exponentials

using a maximum likelihood technique (Colquhoun & Sigworth, 1983; Blatz & Magleby, 1986). Intervals with durations less than about two times the dead time were not included in these fits because durations of such intervals are highly corrupted due to the limited recording bandwidth.

The likelihood ratio test (Rao, 1973; Horn & Lange, 1983; McManus & Magleby, 1988) was used to determine the number of exponential components required to satisfactorily fit the dwell time distributions of open and closed intervals with a level of significance of 0.01.

#### *Single-channel kinetic stability*

In order to assess the stability of single-channel gating kinetics, running means of open intervals were calculated for all data sets (Blatz & Magleby, 1986; McManus & Magleby, 1988; Weiss & Magleby, 1990). The mean duration of the first fifty sequential open intervals was calculated and plotted against interval number, then the mean of the next fifty intervals was calculated and plotted, and so on until all of the 10000–500000 intervals were used. The final 'stability' plot always exhibits fluctuations of the running mean about the overall or 'grand mean' due to the stochastic nature of single-channel kinetics. The degree of these fluctuations remains constant during periods when channel kinetic behaviour is constant. Averaging small numbers of intervals at a time gives one indication of the short-term stability of channel data, while using larger numbers of intervals in each running mean gives information about the long-term stability. Plots of running means of closed intervals are less informative than open intervals plots, due to the much larger normal variation in the closed interval durations. As shown in Results, and mentioned in Weiss & Magleby (1990), stability plots can also indicate the presence of subconducting channel states.

Results are presented as means  $\pm$  s.e.m., with the number of individual membrane patches in which the observation was made at least once as the number of observations ( $n$ ).

## RESULTS

### *Identification of neuronal fast Cl<sup>-</sup> channels*

Neuronal fast Cl<sup>-</sup> channels exhibited some properties that were similar to those of fast Cl<sup>-</sup> channels in tissue-cultured skeletal muscle. Figure 1 presents single-channel currents from an excised, inside-out neuron membrane patch containing a single active Cl<sup>-</sup> channel. Both the formerly intracellular and extracellular membrane surfaces were bathed in identical solutions containing 140 mM-KCl. At large positive potentials currents are outward as indicated by the upward current deflections and the channel spends most of the time in the open state, with brief flickers into the shut state. As the membrane potential is held at less positive values both the current magnitude and the percentage of time the channel is open decreases until, at around zero millivolts, the current changes direction and becomes inward. For the particular channel shown in Fig. 1, a linear regression through the currents from -40 to 90 mV gave a single-channel conductance of 62 pS. For five additional channels under similar conditions the single-channel conductance was  $62 \pm 2.3$  pS. The current-voltage relationship was nearly linear within the examined voltage range. To enhance the signal-to-noise ratio, and to reduce contamination of Cl<sup>-</sup> currents with currents from K<sup>+</sup> channels, the majority of recordings for this study were obtained with the formerly intracellular membrane surface bathed with a solution containing 1 M-KCl and the formerly extracellular membrane surface bathed in 140 mM-KCl. The use of these solutions was advantageous for two main reasons: first, the high intracellular Cl<sup>-</sup> concentration increased the single-channel conductance and the driving force on chloride ions, allowing the stable high resolution recordings required for analysis. Second, K<sup>+</sup> currents were eliminated at membrane potentials near the potassium equilibrium potential of -45 mV.

Currents through a single active fast  $\text{Cl}^-$  channel bathed in asymmetric solutions at different membrane potentials are shown in Fig. 2A with the single-channel current-voltage relationship presented in Fig. 2B. Also in Fig. 2B is shown the current-voltage relationship of a channel bathed in symmetric 140 mM-KCl. Under

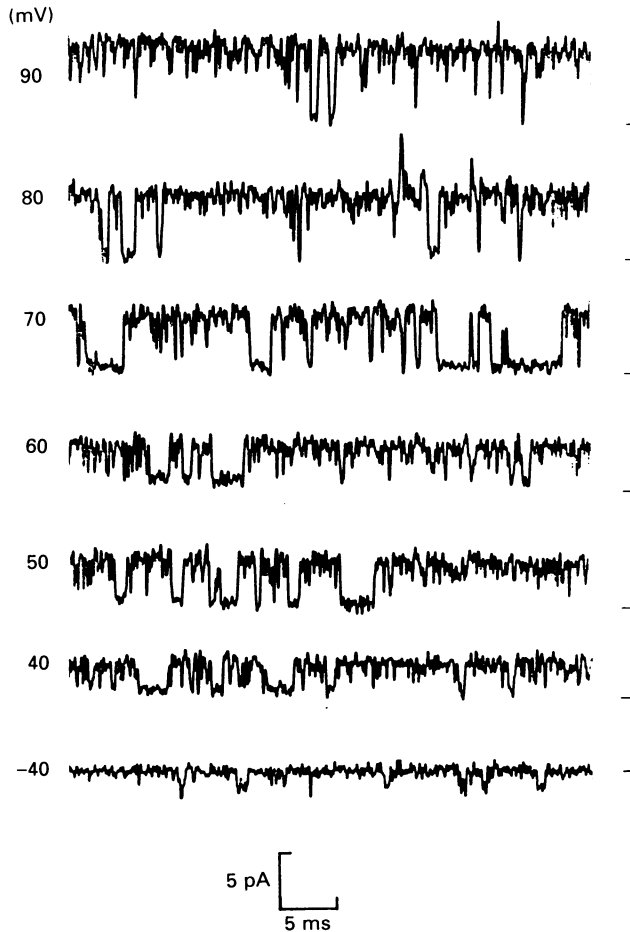


Fig. 1. Single-channel currents through neuronal fast  $\text{Cl}^-$  channel. Intracellular and extracellular solutions were identical and contained (mM): 140 KCl, 5 TES, 1 EGTA, 1.095  $\text{CaCl}_2$ . In this and all subsequent figures outward currents are depicted as upward deflections in current record. Holding potentials are listed to the left of each current trace and are absolute potentials (not relative to 'resting potential'). Closed channel current level is shown to the right of current traces.

the asymmetric conditions the single-channel conductance was  $146 \pm 5.03$  pS ( $n = 10$ ). The voltage dependence of the percentage time open (described below) is clear from Fig. 2A, with the channel activity decreasing with negative potentials. At large depolarizations large-conductance  $\text{Ca}^{2+}$ -activated  $\text{K}^+$  channels, which have been

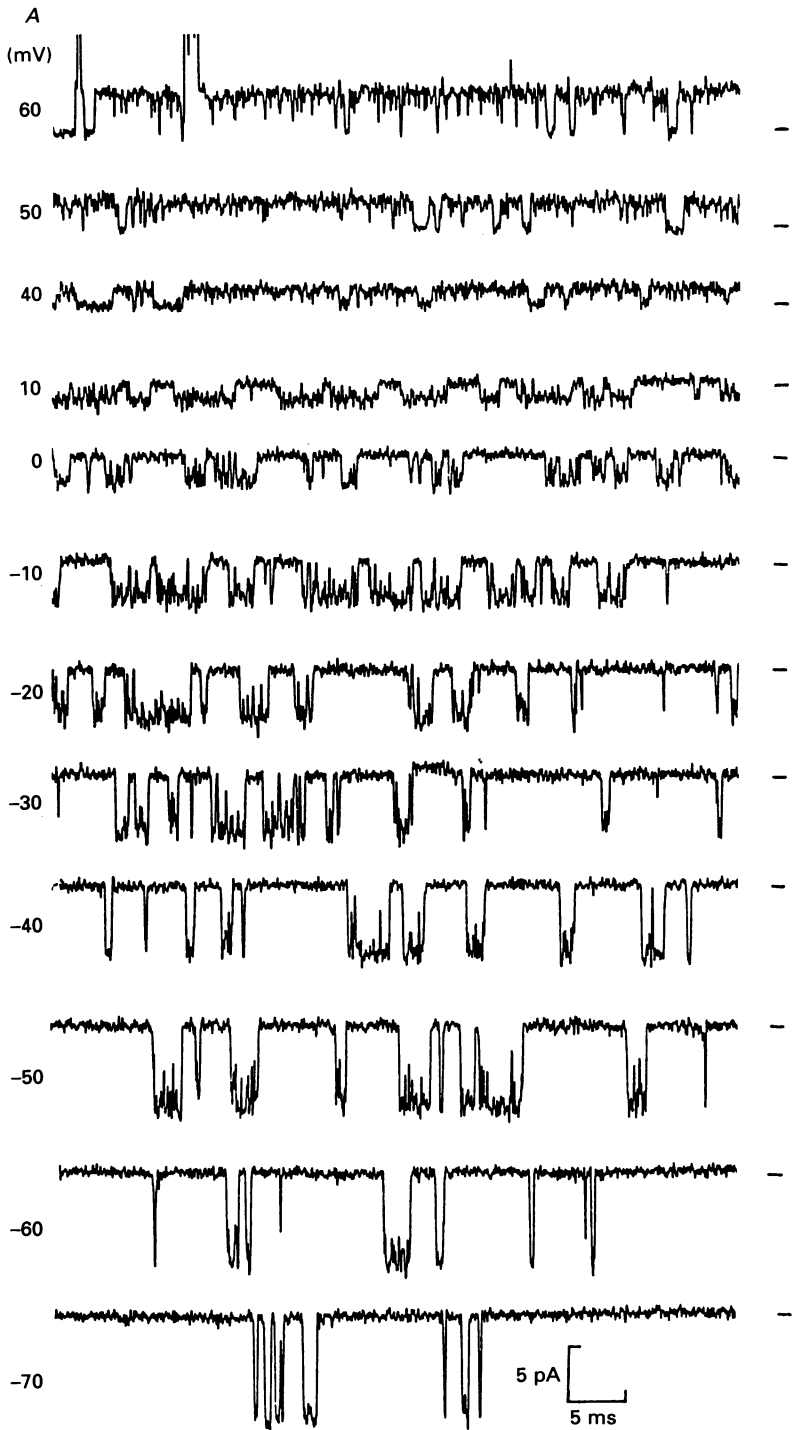


Fig. 2(A). For legend see facing page.

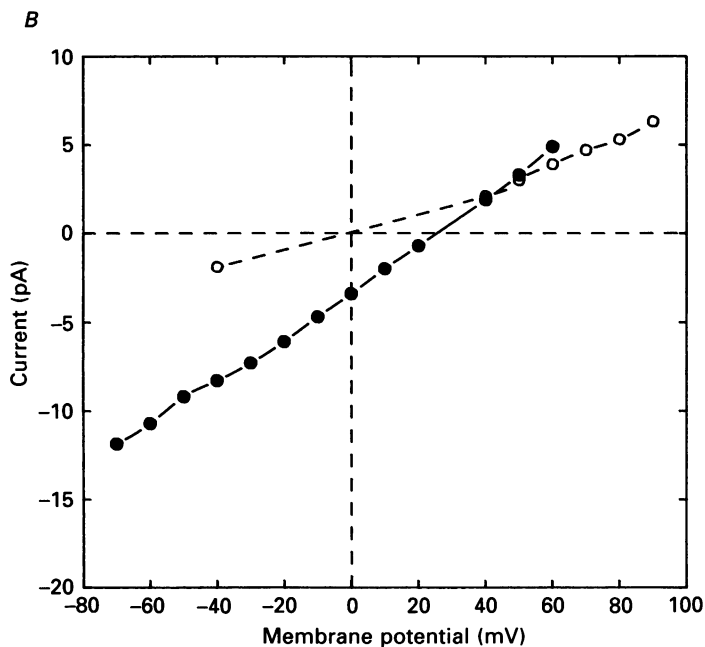


Fig. 2. Current-voltage relationships of fast  $\text{Cl}^-$  channels. *A*, currents through a single  $\text{Cl}^-$  channel at different holding potentials in excised, inside-out membrane patch. Intracellular solution contained 1000 mM-KCl, extracellular solution contained 140 mM-KCl. Holding potentials are listed to left of current traces. Closed channel current level is shown to the right of current traces. Saturating outward channel openings in initial part of 60 mV trace are from large-conductance  $\text{Ca}^{2+}$ -activated  $\text{K}^+$  channels. *B*, single-channel current amplitudes plotted against holding potential. Data were obtained from the same patch bathed in 1000 mM-KCl as in *A* (●, continuous line) or from the same patch with symmetric 140 mM-KCl as in Fig. 1 (○, dashed line). Single-channel conductances obtained by linear regression were 62.0 pS in symmetric 140 mM-KCl and 127.8 pS in 1000 mM-KCl<sub>i</sub>-140 mM-KCl<sub>o</sub>.

shown to be present in these cells (Blatz, 1990*a*) can become activated. These currents appear as attenuated upward transients in Fig. 2*A* at +60 mV, even with the intracellular  $\text{Ca}^{2+}$  concentration buffered by 1 mM-EGTA.

#### *Neuron Cl<sup>-</sup> channels are permeable to cations*

When the intracellular KCl concentration was raised above 140 mM, the reversal potentials of currents through fast  $\text{Cl}^-$  channels shifted from zero to positive potentials as expected for channels that were permeable predominantly to  $\text{Cl}^-$  over  $\text{K}^+$ . The expected reversal potential (taking activity coefficients into account) for perfectly selective  $\text{Cl}^-$  channels under asymmetrical 1 M-140 mM-KCl conditions would be +44 mV. Under these conditions, fast  $\text{Cl}^-$  channel currents reverse at  $+25.3 \pm 0.33$  mV ( $n = 10$ ), much less positive than expected for a channel perfectly selective for  $\text{Cl}^-$ . Based on this shift in reversal potential the permeability ratio of  $\text{Cl}^-$  to  $\text{K}^+$ ,  $P_{\text{Cl}}/P_{\text{K}}$  is calculated to be  $4.8 \pm 0.2$  with the Goldman-Hodgkin-Katz voltage equation (Goldman, 1943; Hodgkin & Katz, 1949; Franciolini & Nonner, 1987). The less than ideal shift in reversal potential of  $\text{Cl}^-$  channel currents is not due

to errors in potential measurement or solution composition as large-conductance  $\text{Ca}^{2+}$ -activated  $\text{K}^+$  channels, which are known to be perfectly selective for cations over  $\text{Cl}^-$  in tissue-cultured skeletal muscle (Blatz & Magleby, 1984), exhibit a reversal potential of  $-45 \pm 0.86$  mV ( $n = 10$ ) in neurons under identical conditions (not shown). This measurement ensures that incorrect solutions, command potential, or junction potential errors are not responsible for the less than ideal shifts in reversal potentials for neuron fast  $\text{Cl}^-$  channels. Measurements of reversal potential shifts when the channels were bathed with 1 M-NaCl (not shown) indicated that  $\text{Na}^+$  was approximately as permeant as  $\text{K}^+$  through these channels. A striking observation is the linearity of the current-voltage relationship of the fast  $\text{Cl}^-$  channels in the presence of the large asymmetric  $\text{Cl}^-$  ion concentrations (Fig. 2B). This phenomenon is possibly due to the presence of outward rectification of single-channel current observed at more positive potentials than presented in this study (A. L. Blatz, unpublished observation). If the channel passes outward current more rapidly than inward current, this could compensate for the expected rectification due to the asymmetric solutions.

#### *Kinetic activity of neuron $\text{Cl}^-$ channels*

Fast  $\text{Cl}^-$  channels were active at all examined membrane potentials between  $-90$  and  $+80$  mV. Figure 3A presents currents recorded during a 1 min period from an excised, inside-out membrane patch containing a single active  $\text{Cl}^-$  channel that was held at  $-40$  mV while bathed with the standard asymmetrical [KCl] solutions. In this particular recording, the single fast  $\text{Cl}^-$  channel did not appear for 10 min following excision of the patch into the high- $\text{K}^+$  solution. The four traces are not contiguous and each represents about 16 s of recording time. Single  $\text{Cl}^-$  channel currents are presented in Fig. 3B at three higher levels of time resolution. It is apparent from Fig. 3 that neuron fast  $\text{Cl}^-$  channel gating activity is complex and occurs in the form of bursts (or clusters of bursts) of rapid open and closed intervals (which in Fig. 3A appear as horizontal bars due to the low time resolution) separated by closed intervals of longer durations. The current traces in Fig. 3A also illustrate the stability of the recordings which is a requirement for subsequent analysis. Clusters of channel activity are themselves composed of bursts of activity separated by longer closures, and, even at the highest resolution, the open events are not discrete openings, but are composed of one or more brief closing events (Fig. 3B). Analysed in terms of traditional Markovian assumptions, this range of closed intervals suggests that the kinetic scheme underlying  $\text{Cl}^-$  channel activity contains a variety of closed kinetic states with mean lifetimes ranging from microseconds to seconds. The open channel intervals, on the other hand, are much more consistent in duration, clustering around 1 ms, with no extremely long or short open intervals. This suggests that fewer open kinetic states will be required to account for the channel's open intervals.

#### *Stability of neuron fast $\text{Cl}^-$ channel kinetic activity*

Neuron fast  $\text{Cl}^-$  channels did not exhibit 'run-down' or 'wash-out' effects that have been demonstrated for other ion channels. Current records obtained at the beginning of a recording session (after channels became active) were essentially



identical to those obtained several hours later, even after constant perfusion with high and/or low ionic strength solutions. As shown below, however, alterations of kinetic activity do occur during the course of an experiment.

*Neuronal Cl<sup>-</sup> channels exhibit different modes of kinetic activity*

*Normal mode*

The vast majority of neuron Cl<sup>-</sup> channel activity was made up of open and closed intervals similar to those presented in Fig. 3. During this 'normal mode' of activity,

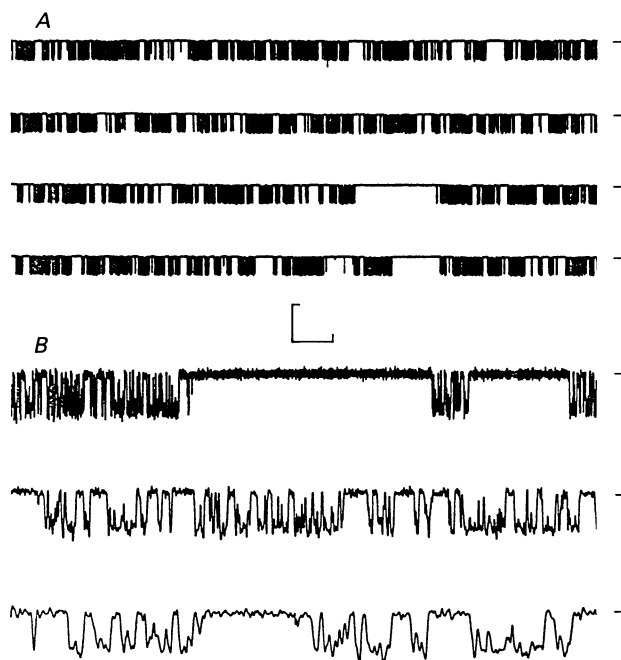


Fig. 3. Single-channel Cl<sup>-</sup> currents at low (*A*) and high (*B*) levels of time resolution. Inside-out membrane patch was held at  $-40$  mV in asymmetric solutions (1000 mM-KCl<sub>i</sub>, 140 mM-KCl<sub>o</sub>). Closed channel current is shown to the right of current traces. Current calibration bar is 20 pA for *A* and 10 pA for *B*. Time calibration bar represents 1.12 s for *A*, and 1.86 ms, 4.65 ms and 18.62 ms for top, middle and bottom trace in *B*, respectively. Currents were filtered with a cut-off frequency of 300 Hz for *A* and 3.2 kHz for *B*.

the mean open and closed durations averaged about 0.3–0.5 and 2.0–3.0 ms, respectively, at a holding potential of  $-40$  mV. In order to carry out the analysis of open and closed dwell times it is necessary for the single-channel data to be stable. One method of assessing this stability of kinetic activity is with the running mean open interval or stability plots, constructed as described in the Methods. Running mean plots of 100000 open intervals from three patches, each containing a single Cl<sup>-</sup> channel, are shown in Fig. 4. These three channels are representative of the typical stability of neuronal fast Cl<sup>-</sup> channels, in that the running mean remained stable throughout most of the recording. An example of an occasional finding is illustrated in Fig. 4*C*, where the running mean plot remained stable during part of the

recording, and then shifted, over the course of several thousands of intervals, to a new stable value. Blatz & Magleby (1986) and Weiss & Magleby (1990) have demonstrated that simple kinetic models predict the short-term variation of running means about the overall mean. The degree of this variation is dependent on the

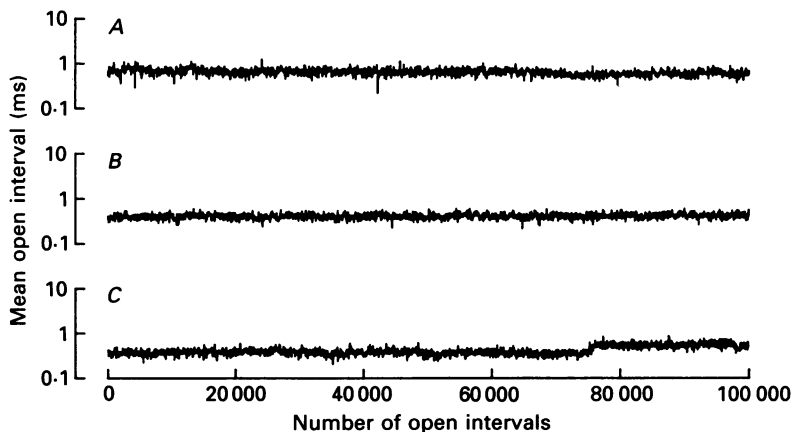


Fig. 4. Running mean open plots (stability plots) for three different fast  $\text{Cl}^-$  channels. For each plot, the first fifty open intervals were averaged and plotted against interval number, then the next fifty intervals were averaged and plotted, and so on until all 100 000 open intervals for each channel were averaged and plotted. Note that  $y$ -axes are logarithmic. Slow drift in plot *C* is real and cannot be explained by drifts in membrane potential or other artifacts.

number of intervals used for each running mean. The source of the shift to longer durations of mean open duration is not clear at this time. A similar shift of mean open duration was reported by Weiss & Magleby (1990) for tissue-cultured muscle  $\text{Cl}^-$  channels.

#### *Inactivated mode*

Neuron fast  $\text{Cl}^-$  channels are rarely observed to be active in cell-attached membrane patches under the conditions of these experiments. Currents through these channels are only seen following excision of the patch from the cell. Additionally, after the channels have become activated, they often become inactive for several seconds to tens of minutes, and then return to normal activity. Blatz & Magleby (1986) refer to this phenomenon as the channel entering and leaving an 'inactivated' mode. As is the case with tissue-cultured skeletal muscle, insufficient numbers of excursions into this mode occur to allow its detailed analysis in neuronal  $\text{Cl}^-$  channels.

#### *Buzz mode*

Although the vast majority of  $\text{Cl}^-$  channel kinetic activity occurred during the 'normal mode', with mean open and closed interval durations of about 0.3–0.5 and 2.0–3.0 ms, respectively, occasionally (less than 0.1% of the total number of intervals), the mean intervals both suddenly decreased. An example of this mode of

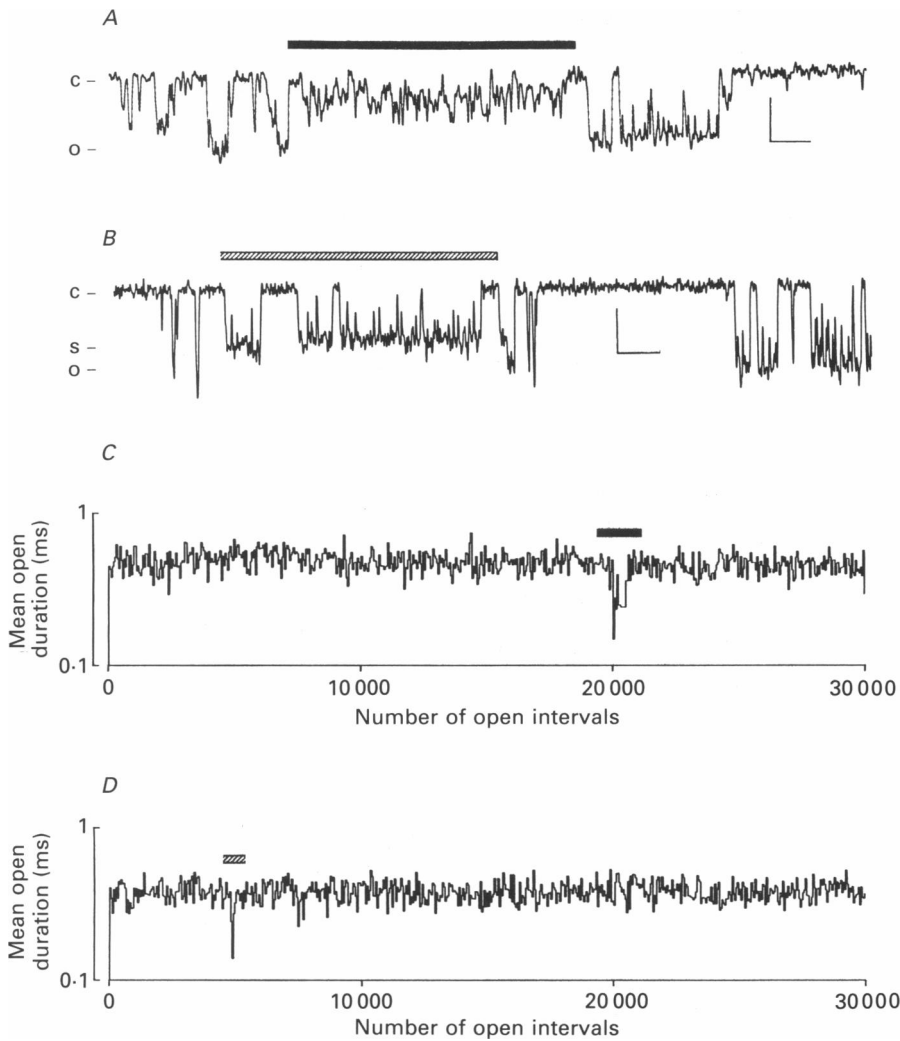


Fig. 5. Two different modes of activity of neuronal fast Cl<sup>-</sup> channels. *A* and *B*, single-channel current records of different channels that entered the buzz mode (*A*) or the subconductance mode (*B*). Filled bar over current trace in *A* indicates when this channel entered the buzz mode. Hatched bar over current trace in *B* indicates when this channel entered the subconductance mode. Fully open (o) subconducting (s) and fully-closed (c) levels are indicated to the left of the current traces in *A* and *B*. Currents were filtered at 3.2 kHz and sampled at 100  $\mu$ s per point. Current amplitude and time calibration bars in *A* and *B* represent 4 pA and 3.5 ms, respectively. *C* and *D*, running mean (fifty intervals per mean) plots of intervals recorded from channels in *A* and *B* during periods when channels entered buzz and subconductance modes. Entry into the buzz mode is indicated by a filled bar over the running mean plot in *C*. Entry into the subconducting mode is indicated in *D* by the hatched bar over the running means.

activity is shown in Fig. 5*A*. About 100 000 open and closed events were recorded from a single fast Cl<sup>-</sup> channel held at -40 mV. During most of this period, the channel exhibited activity similar to that shown in Fig. 3. After about 1 min of

recording, the durations of the open intervals fell sharply. During this mode of activity, indicated in Fig. 5A by the filled bar above the current trace, the amplitude of the individual current steps appeared to decrease, but this is most probably due to the attenuation of complete open and closed events by limited time resolution due to the required filtering. This period of abnormal activity lasted about 20 ms and involved about fifty open and closed intervals. The channel can leave the buzz mode for a period, return to normal mode, and then return to the buzz mode. This behaviour typically occurs during a period of several seconds and then disappears for several minutes. Often only one occurrence of the buzz mode is observed during the entire recording period. Intervals during the buzz mode of activity were located by eye during the digitizing of the experimental record, and excluded at that time, or removed after examining stability plots (see above) where their presence was usually indicated by a drop in the running open interval means (indicated in Fig. 5C as the filled bar above the running means).

#### *Neuron Cl<sup>-</sup> channels enter subconductance states*

At room temperature neuron Cl<sup>-</sup> channels also rarely entered another form of activity where the channel opened between the fully closed current level and a current level about two-thirds of the normal open current level. Such a period of activity from another patch is shown in Fig. 5B. During this period, indicated by the hatched bar above the current trace, the channel opened and closed between the fully closed and open conductance state for several seconds and then, for about 15 ms opened and closed between the fully closed conductance state and a subconductance state of 98 pS. The kinetics during the subconductance mode were similar to the normal mode kinetics, although insufficient numbers of intervals were obtained for a detailed analysis. Excursions into this mode of activity could be detected in the running mean plots as an apparent drop in the mean open interval durations as indicated by the hatched bar in Fig. 5D. The current record and running mean plots were examined and events during subconductance modes were not included in the detailed kinetic analysis of dwell times. Entries into the subconductance mode of activity which lasted for only a few open intervals could not be detected with the running mean plots, but an interval-by-interval scanning of the current traces used in the analysis did not indicate that this mode of activity was entered often enough to influence the final results. At colder experimental temperatures the durations of excursions into both the buzz mode and the subconductance mode were increased (data not shown).

#### *Distributions of open and shut intervals*

Fast Cl<sup>-</sup> channels from cortical neurons exhibit complex steady-state kinetic activity. Figure 6 presents a typical distribution of open intervals from a single Cl<sup>-</sup> channel recorded at -40 mV. The continuous line in Fig. 6 is the best fit of two exponential components to the open interval distribution including intervals from 0.062 to 10 ms. This fit gives an excellent description of the distribution of open intervals. Based on the likelihood ratio test, two exponential components fitted the data better than a single component and three components did not improve the fit over two (likelihood ratios for two exponential components *vs.* one was 637, and for

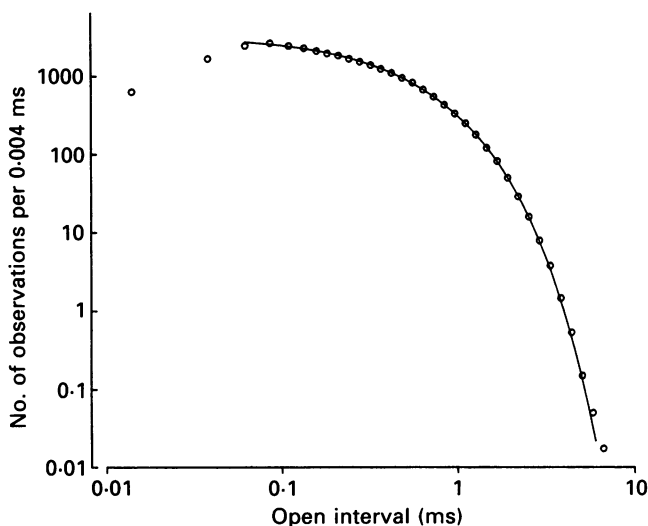


Fig. 6. Distribution of open interval durations for a single fast  $\text{Cl}^-$  channel (channel 1 in Tables 1 and 2). Double logarithmic plot of all open intervals recorded from excised, inside-out membrane patch held at  $-40$  mV. Continuous line is the best fit of the sum of two exponential components (with values listed in Table 1) to open interval distribution. Open intervals with durations less than  $0.062$  ms were not included in the fits as they are corrupted by the limited recording bandwidth. Dead time of  $0.03$  ms.

TABLE 1. Observed distributions of open intervals  
Time constants and relative areas

	Channel 1		Channel 2		Channel 3	
Component	$\tau$ (ms)	Area (%)	$\tau$ (ms)	Area (%)	$\tau$ (ms)	Area (%)
1	0.255	26.7	0.295	32.1	0.263	13.8
2	0.530	73.3	0.407	67.9	0.672	86.2

Time constants ( $\tau$ ) and relative areas are the best fit to two exponential components to open intervals with durations greater than  $0.062$  ms. Membrane potential of  $-40$  mV. Numbers of analysed open events were: 283375 (channel 1), 110855 (channel 2), and 113501 (channel 3). Dead time of  $0.03$  ms. Open interval distribution for channel 1 is presented in Fig. 6.

three components *vs.* two was 2.8). For the three patches containing single  $\text{Cl}^-$  channels that were analysed in detail, all exhibited open interval distributions that were best fitted by sums of two exponentials with time constants and areas given in Table 1. This result suggests that, during normal activity, neuron  $\text{Cl}^-$  channels enter at least two open kinetic states.

The distributions of closed interval durations were more complex, as shown in Fig. 7. Closed interval durations were fitted to sums of exponentials including durations from  $0.062$  ms to 1–2 s. This range of durations included all closed channel events except for the few extremely long events which represent entry of the channel into the inactivated mode. The continuous line in Fig. 7 is the best fit of the data to the sum of six exponential components. The sum of six components fitted the data

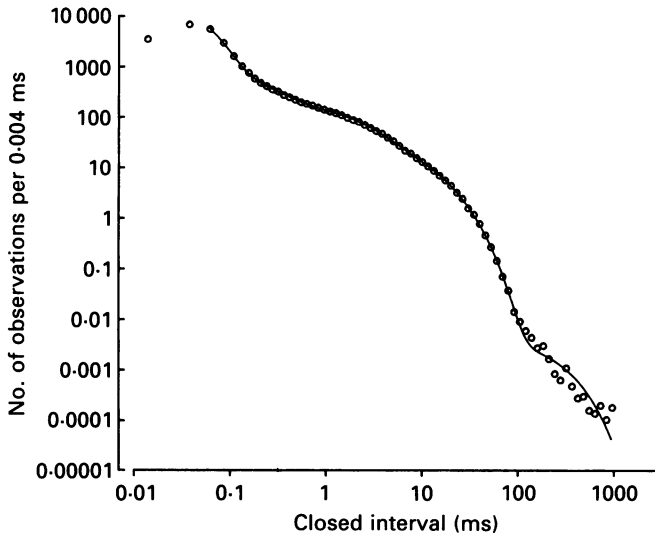


Fig. 7. Distribution of closed interval durations for a single fast  $\text{Cl}^-$  channel (same channel as in Fig. 6). Double logarithmic plot of all closed intervals recorded from excised patch held at  $-40$  mV. Continuous line is the best fit sum of six exponential components (values listed in Table 2). Closed intervals with durations between 0.062 and 1000 ms were included in this fit. Intervals with durations less than 0.062 ms were not included because they were corrupted by the limited recording bandwidth. Dead time of 0.03 ms.

TABLE 2. Observed distributions of closed intervals  
Time constants and relative areas

Component	Channel 1		Channel 2		Channel 3	
	$\tau$ (ms)	Area (%)	$\tau$ (ms)	Area (%)	$\tau$ (ms)	Area (%)
1	196.5	0.05	161.0	0.005	250.2	0.137
2	13.2	9.28	8.93	6.45	46.1	0.30
3	6.45	8.79	5.93	8.38	7.40	1.84
4	1.80	15.19	1.36	17.8	2.21	13.0
5	0.179	7.39	0.142	10.4	0.758	12.0
6	0.0295	59.3	0.0266	57.0	0.160	6.32
7	—	—	—	—	0.025	66.4

Time constants ( $\tau$ ) and relative areas are the best fit sums of six (channels 1 and 2) or seven (channel 3) exponential components to closed intervals with durations between 0.062 and 1000 ms (channel 1) or 2000 ms (channels 2 and 3). Membrane potential of  $-40$  mV. Numbers of analysed closed events were: 223702 (channel 1), 89516 (channel 2), and 81725 (channel 3). Dead time of 0.03 ms. Closed interval distribution for channel 1 is plotted in Fig. 7.

significantly better, based on the likelihood ratio criterion, than the sum of five components and fitting the data to the sum of seven exponentials, in this case, did not provide a significantly superior fit (likelihood ratio of six exponential components *vs.* five was 58 and for seven components *vs.* six was 2.22). Time constants and areas of the best fit sums of exponentials are shown in Table 2 for the three analysed patches. This result suggests that, during normal activity, the neuron  $\text{Cl}^-$  channel

enters at least six and sometimes seven kinetic states with mean lifetimes ranging from microseconds to hundreds of milliseconds. In all cases where sufficient numbers of open and closed events were recorded, two exponential components were required to adequately fit the open interval distribution and six or seven exponentials were required to fit the closed interval distributions.

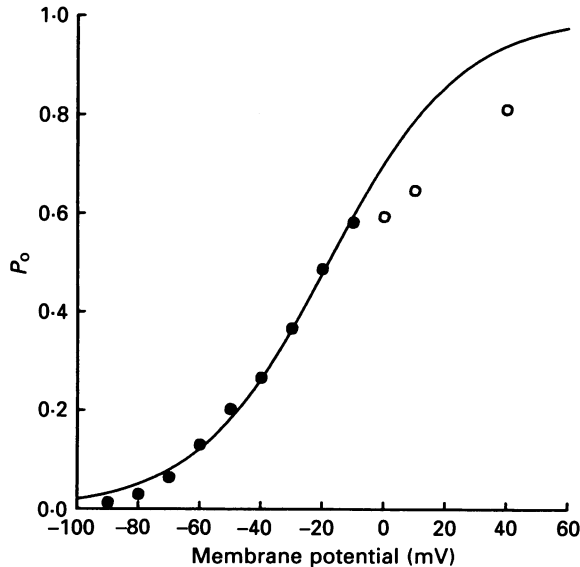


Fig. 8. Voltage dependence of open time probability ( $P_o$ ) for a neuronal fast  $\text{Cl}^-$  channel. Open and closed interval durations were obtained as described in Methods using a 50% threshold criterion. At least 16000 events were recorded at each potential.  $P_o$  was calculated at each membrane potential as the total duration of the recorded open intervals divided by the sum of the open and closed intervals. Filled circles (●) were obtained from currents filtered at 6.2 kHz. Open circles (○) were obtained from currents filtered at 3.97 kHz to reduce noise to acceptable levels, and are therefore not directly comparable with the data obtained with less filtering. Only the filled circles were used to fit eqn (1) to the observed data. The continuous line is the best fit (least squares criterion) of eqn (1) to the filled circles.

#### *Voltage dependence of neuron fast $\text{Cl}^-$ channel gating*

Neuron fast  $\text{Cl}^-$  channels are affected by membrane potential in a complex manner. As presented in Figs 1 and 2, the percentage of time a channel spends in the open state increases with increasing membrane depolarization. The open probability ( $P_o$ ) plotted against membrane potential is presented in Fig. 8A. In this case,  $P_o$  increased with depolarization from  $-90$  to  $-20$  mV. As the patch was further depolarized  $P_o$  increased less rapidly. At least part of the reason that the increase in  $P_o$  slowed down as the membrane potential was made more positive than about  $-10$  mV was the increased occurrence of long-lived closed intervals, with durations much longer than could be accounted for by the six or seven exponential components of the closed dwell time distributions presented above. Analysis of  $\text{Cl}^-$  channel

currents at potentials more positive than about  $-20$  mV was difficult for three reasons. First, contamination of the current record from other channels occurred more often at positive potentials. Second, open and closed gating activity was complicated by the increased numbers of excursions into the inactivated mode. Third, in almost all experiments, positive potentials would cause the activation of additional fast  $\text{Cl}^-$  channels that had been in the membrane patch but inactive. This recruitment of  $\text{Cl}^-$  channels by depolarization was a very common phenomenon and usually prevented dwell time analysis at depolarized potentials. For these reasons, the further analysis of the voltage dependence of  $\text{Cl}^-$  channel activity was performed at membrane potentials between  $-90$  and  $-10$  mV. Within this voltage range the relationship between open time probability and membrane potential is fairly well fitted (continuous line in Fig. 8) by

$$P_o = 1/[1 + \exp(-q(V - V_{0.5})/kT)], \quad (1)$$

where  $q$  is the effective gating charge and  $V_{0.5}$  is the potential at which  $P_o$  is 0.5, and  $k$  and  $T$  have their usual meanings. This equation describes the expected voltage dependence of a two-state open-closed channel model (cf. Hodgkin & Huxley, 1952; Hille, 1984; Weiss & Magleby, 1990). Since it has already been shown above that fast  $\text{Cl}^-$  channel kinetic activity cannot be described in terms of such a simple model the values of  $q$  and  $V_{0.5}$  should be used only for comparison with other channels and eqn (1) should not be used to imply a mechanism for voltage dependence. The steepness of the relationship between membrane potential and  $P_o$  was fairly constant among  $\text{Cl}^-$  channels ( $q = 1.28 \pm 0.100$ ,  $n = 3$ ), but the  $P_o$  curve was shifted along the voltage axis by various amounts for different channels ( $V_{0.5} = -18.10 \pm 11.95$  mV,  $n = 3$ ). One complication of this analysis is that the values obtained for  $V_{0.5}$  were highly dependent on which points were chosen for analysis. Choosing values for  $P_o$  obtained at the most negative potentials (which were the most accurately measured as the signal-to-noise ratio was the highest) resulted in a negative shift in the fitted curve and therefore a more negative value for  $V_{0.5}$ . A similar lack of a good fit of eqn (1) to  $P_o$  in muscle  $\text{Cl}^-$  channel data is evident in Fig. 6 of Weiss & Magleby (1990).

The observed increase of  $P_o$  with positive membrane potential could be the result of a change in either mean open duration or mean closed duration. Figure 9 plots the mean open and closed durations against membrane potential for the same channel as in Fig. 8. Mean open duration was relatively unaffected by membrane potential within the tested range of  $-90$  to  $-10$  mV. The slope of the linear regression through the logarithm of the mean open durations indicates a small voltage dependence of an e-fold change in mean open duration for 952 mV change in membrane potential for this particular channel (mean value for three channels: e-fold change per 1143 mV change in membrane potential  $\pm 367$  mV). The mean closed duration, on the other hand, was extremely sensitive to membrane potential, as demonstrated by the open squares ( $\square$ ) in Fig. 9. For this channel, the mean closed duration decreased from over 40 ms at  $-90$  mV to less than 1 ms at  $-10$  mV. A linear regression through the logarithm of the mean closed durations indicates a large voltage dependence of an e-fold decrease in mean closed duration for a 39 mV depolarization for this channel (e-fold change per  $38 \pm 1.6$  mV,  $n = 3$ ). Thus, the increase in  $P_o$  with depolarization is almost totally due to a decrease in the mean



closed duration. The open durations are relatively unaffected by membrane potential. A somewhat confusing result is that an 'effective gating charge' of 1.3 can be calculated from the  $P_o$  vs. voltage relationship. If all (or most) of the voltage dependence of channel gating is caused by a decrease in mean closed duration (Fig.

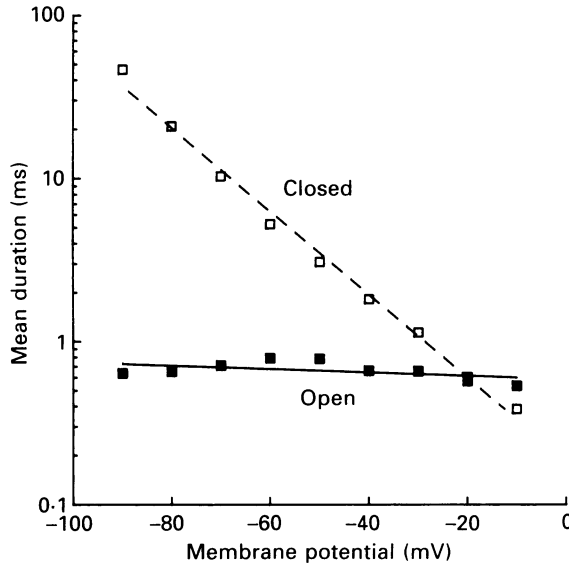


Fig. 9. Voltage dependence of neuron fast  $\text{Cl}^-$  channels is due mainly to the voltage dependence of mean closed durations. Semilogarithmic plot of mean open durations (■) and mean closed durations (□) obtained from same current recording as in Fig. 8. All mean durations were obtained from current records filtered at 6.2 kHz. Continuous line through filled squares is the best fit linear regression to the logarithm of the mean open durations vs. membrane potential. Dashed line through open squares is the best fit regression to the logarithms of the mean closed durations. Regression parameters are given in text.

9) then the 'effective gating charge' calculated from the mean closed interval durations vs. voltage should equal that calculated from the  $P_o$  data. In fact, the value obtained is larger (1.5) confirming that the simple two-state kinetic model assumed in the calculation of 'effective gating charge' is not correct.

#### DISCUSSION

This study demonstrates the presence of fast  $\text{Cl}^-$  channels in acutely dissociated rat cerebral cortical neurons. These  $\text{Cl}^-$  channels share some properties with fast  $\text{Cl}^-$  channels found previously only in tissue-cultured embryonic-derived cells.

#### *Conductance properties of neuron fast $\text{Cl}^-$ channels*

Fast  $\text{Cl}^-$  channels from cortical neurons are permeable to at least two cations,  $\text{Na}^+$  and  $\text{K}^+$ , as well as to  $\text{Cl}^-$  ions. This finding is consistent with results from  $\text{Cl}^-$  channels from other tissues and seems to be a general property of anion channels. Franciolini

& Nonner (1987) found that smaller-conductance  $\text{Cl}^-$  channels from tissue-cultured rat hippocampus were also permeable to a number of cations, with permeability ratios similar to those reported in this study. Larger-conductance  $\text{Cl}^-$  channels from cultured hippocampal neurons also exhibited a measurable cation permeability (Franciolini & Petris, 1988). Fast- and slow-type  $\text{Cl}^-$  channels and large-conductance  $\text{Cl}^-$  channels from tissue-cultured rat skeletal muscle are also permeable to  $\text{K}^+$  and  $\text{Na}^+$ , based on reversal potential shift measurements (Blatz & Magleby, 1983, 1985).

#### *Modes of kinetic activity of neuron fast $\text{Cl}^-$ channels*

Analysis of neuron fast  $\text{Cl}^-$  channel open and closed interval durations over long periods of time indicates that these channels spend most of the time in what has been called the 'normal' mode of activity by Blatz & Magleby (1986) and Weiss & Magleby (1990). In this normal mode of activity the mean open and closed interval durations are 0.5 and 2.8 ms, respectively, and these mean durations remain constant for tens to hundreds of thousands of events over time periods of several minutes.  $\text{Cl}^-$  channels occasionally enter one or all three alternative gating modes: inactivated mode, buzz mode, or subconductance mode. The observation that kinetic behaviour of single ion channels can alternate between different modes of activity has been made in several different types of channels (Patlak, Gration & Usherwood, 1979; Hess, Lansman & Tsien, 1984; Blatz & Magleby, 1986; McManus & Magleby, 1988; Weiss & Magleby, 1990).

The inactivated mode is the least well-defined of the activity modes. During this mode the channel is closed for long periods of time that cannot be accounted for by even the longest of the six or seven components of the closed dwell time distributions. Of course, it cannot be ruled out that the 'inactivated mode' actually represents an additional closed state from the normal mode of activity that has an extremely long lifetime.

The buzz mode of channel activity occurs only about once per 100 000 open and closed events, or about once every 10 min. During this activity mode the mean open and closed interval durations fall from the normal values to about 0.1 and 0.2 ms, respectively. The transitions between the open and closed current levels may appear to be incomplete due to large amounts of filtering, but as the low-pass corner frequency is increased, the currents can be seen to pass between the completely open and completely closed current levels. This mode of activity has been previously observed only in fast  $\text{Cl}^-$  channels and large-conductance  $\text{Ca}^{2+}$ -activated  $\text{K}^+$  channels from tissue-cultured rat myotubes (Blatz & Magleby, 1986; McManus & Magleby, 1988; Weiss & Magleby, 1990).

Entries into the subconductance mode of activity can be clearly differentiated from entries into the buzz mode of activity as, in the subconductance mode, the single-channel current passes between the fully closed level and a current level about two-thirds the normal mode level. Increasing the corner frequency of the low-pass filter does not increase the amplitude of the current events, indicating that the subconductance level is not due to excessive filtering of the data. Subconductance levels are now a common and normal feature of most ion channels studied at the single-channel level. (GABA)-activated  $\text{Cl}^-$ -selective channels in particular seem to exhibit these subconductance levels, although GABA-activated  $\text{Cl}^-$  channels appear

to enter subconductance modes far more frequently than do the fast  $\text{Cl}^-$  channels reported here (Bormann, Hamill & Sakmann, 1987).

During the majority of time, neuron fast  $\text{Cl}^-$  channels exist in the normal mode of activity. Maximum likelihood fitting techniques have revealed that, during this normal activity the channel enters at least two open kinetic states and at least six or seven closed kinetic states. The mean lifetimes of the closed states span durations from tens of microseconds to hundreds of milliseconds. The mean lifetimes of the open states are much more consistent at around 0.2–0.8 ms. Most ion channels studied in any detail have been found to behave in a manner consistent with an underlying kinetic mechanism containing multiple open and closed kinetic states. Fast  $\text{Cl}^-$  channels in tissue-cultured rat skeletal muscle also exhibit two or three open and at least six closed kinetic states during normal activity (Blatz & Magleby, 1986; Weiss & Magleby, 1990). The time constants and areas of the exponential components fitted to the open and closed distributions of neuron intervals are similar to those reported for fast  $\text{Cl}^-$  channels in tissue-cultured skeletal muscle by Weiss & Magleby (1990), although, in the neuron channels, the relative area of the second fastest component of the closed interval distribution is usually less than that reported by Weiss & Magleby (1990). It is actually quite remarkable that the open and closed interval distributions are so similar for the two channels in two entirely different tissues. This similarity, plus the similarities in cation permeability and voltage dependence, strongly suggests that fast  $\text{Cl}^-$  channels in neuronal tissues and in skeletal muscle are very closely related, if not in fact the same channel.

#### *Voltage dependence of neuron fast $\text{Cl}^-$ channel gating*

Neuronal fast  $\text{Cl}^-$  channel gating is dependent on membrane potential, with the percentage of time the channels are open increasing with membrane depolarization. The major effect of membrane potential is on the mean closed duration, with the mean open duration relatively unaffected by voltage. Absolute values for the degree of voltage sensitivity of the neuron fast  $\text{Cl}^-$  channels are similar to those found in tissue-cultured skeletal muscle. In both muscle and neuron  $\text{Cl}^-$  channels, the major voltage dependence is in the closed durations, with the open interval durations being much less dependent on membrane potential. As discussed by Weiss & Magleby (1990), the voltage sensitivity found for fast  $\text{Cl}^-$  channels is less than that of the  $\text{Na}^+$  and  $\text{K}^+$  channels responsible for the action potential, but greater than most chemically modulated channels.

#### *Possible functions of fast $\text{Cl}^-$ channels*

The function of neurotransmitter-activated  $\text{Cl}^-$  channels in neurons is clearly to hyperpolarize the cell membrane or to increase the membrane conductance to inhibit depolarization by excitatory synaptic input. The function of  $\text{Cl}^-$  channels that are not activated by known neurotransmitters, such as the fast  $\text{Cl}^-$  channel described in this study, is less clear. The fast  $\text{Cl}^-$  channels reported in this study appear to be located in the surface membrane of the dissociated neurons, as GABA-activated  $\text{Cl}^-$  channels, known to be located in the surface membrane (for example, Bormann, Hamill & Sakmann, 1987), can be found in the same membrane patches that contain fast  $\text{Cl}^-$  channels. In acutely dissociated cortical neurons fast  $\text{Cl}^-$  channels are only

rarely observed to be active in cell-attached membrane patches, and, usually, several minutes elapse between the time that the membrane patch is excised from the cell and the appearance of  $\text{Cl}^-$  channels (Blatz, 1990c and A. L. Blatz, unpublished observation). Other types of channels, such as large-conductance  $\text{Ca}^{2+}$ -activated  $\text{K}^+$  channels are active with no delays in cell-attached and excised cortical neuronal patches (A. L. Blatz, unpublished observation). This suggests that fast  $\text{Cl}^-$  channels may not be 'background' channels as defined by Franciolini & Petris (1990) as they do not seem to be active in cell-attached patches under the conditions of these experiments. The absence of cell-attached  $\text{Cl}^-$  channel activity also suggests that these channels may not contribute to the neuronal resting  $\text{Cl}^-$  conductance, although the channels may become inactive during the dissociation process. The delay in activation of the fast  $\text{Cl}^-$  channels following patch excision could suggest that a regulatory component of the channel must be washed away or otherwise modified by excision before the channel can open.

I thank Ken Breedlove, Monya Sigler, and Dorothea Sanchez for technical assistance and for comments on the manuscript. This study was supported by a grant from the NIH (GM 39731).

#### REFERENCES

- BARKER, J. L., HARRISON, N. L. & OWEN, D. G. (1990). Pharmacology and physiology of  $\text{Cl}^-$  conductances activated by GABA in cultured mammalian central neurons. In *Chloride Channels and Carriers in Nerve, Muscle, and Glial Cells*, ed. ALVAREZ-LEEFMANS, F. J. & RUSSELL, J. M., pp. 273–298. Plenum Press, New York.
- BARRETT, J. N., MAGLEBY, K. L. & PALLOTTA, B. S. (1982). Properties of single calcium-activated potassium channels in cultured rat muscle. *Journal of Physiology* **331**, 211–230.
- BLATZ, A. L. (1990a). Large and small conductance  $\text{Ca}$ -activated potassium channels in adult and tissue-cultured rat cerebral cortex neurons. *Biophysical Journal* **57**, 116a.
- BLATZ, A. L. (1990b). Chloride channels in skeletal muscle. In *Chloride Channels and Carriers in Nerve, Muscle and Glial Cells*, ed. ALVAREZ-LEEFMANS, F. J. & RUSSELL, J. M., pp. 407–419. Plenum Press, New York.
- BLATZ, A. L. (1990c). Fast chloride channels are present in most dissociated rat cerebral neurons. *Society for Neuroscience Abstracts* **16**, 668.
- BLATZ, A. L. & MAGLEBY, K. L. (1983). Single voltage-dependent  $\text{Cl}^-$  selective channels of large conductance in cultured rat muscle. *Biophysical Journal* **43**, 237–241.
- BLATZ, A. L. & MAGLEBY, K. L. (1984). Ion conductance and selectivity of single calcium-activated potassium channels in cultured rat muscle. *Journal of General Physiology* **84**, 1–23.
- BLATZ, A. L. & MAGLEBY, K. L. (1985). Single chloride-selective channels active at resting membrane potentials in cultured rat skeletal muscle. *Biophysical Journal* **47**, 119–123.
- BLATZ, A. L. & MAGLEBY, K. L. (1986). Quantitative description of three modes of activity of fast chloride channels from rat skeletal muscle. *Journal of Physiology* **378**, 141–174.
- BLATZ, A. L. & MAGLEBY, K. L. (1989). Adjacent interval analysis distinguishes among gating mechanisms for the fast chloride channel from rat skeletal muscle. *Journal of Physiology* **410**, 561–585.
- BORMANN, J., HAMILL, O. P. & SAKMANN, B. (1987). Mechanism of anion permeation through channels gated by glycine and  $\gamma$ -aminobutyric acid in mouse cultured spinal neurones. *Journal of Physiology* **385**, 243–286.
- BRETAG, A. H. (1987). Muscle chloride channels. *Physiological Reviews* **67**, 618–724.
- COLQUHOUN, D. & SIGWORTH, F. J. (1983). Fitting and statistical analysis of single-channel records. In *Single-Channel Recording*, ed. SAKMANN, B. & NEHER, E., pp. 191–263. Plenum Press, New York.
- FRANCIOLINI, F. & NONNER, W. (1987). Anion and cation permeability of a chloride channel in rat hippocampal neurons. *Journal of General Physiology* **90**, 453–478.

- FRANCIOLINI, F. & PETRIS, A. (1988). Single chloride channels in cultured rat neurons. *Archives of Biochemistry and Biophysics* **261**, 97–102.
- FRANCIOLINI, F. & PETRIS, A. (1990). Chloride channels of biological membranes. *Biochimica et Biophysica Acta* **1031**, 247–259.
- GOLDMAN, D. E. (1943). Potential, impedance, and rectification in membranes. *Journal of General Physiology* **27**, 37–60.
- HAMILL, O. P., MARTY, A., NEHER, E., SAKMANN, B. & SIGWORTH, F. J. (1981). Improved patch-clamp technique for high-resolution current recording from cells and cell-free membrane patches. *Pflügers Archiv* **391**, 85–100.
- HESS, P., LANSMAN, J. B. & TSIEN, R. W. (1984). Different modes of  $\text{Ca}^{2+}$  channel gating behavior favoured by dihydropyridine  $\text{Ca}^{2+}$  agonists and antagonists. *Nature* **311**, 538–544.
- HILLE, B. (1984). *Ionic Channels in Excitable Membranes*. Sinauer Associates Inc., Sunderland, MA, USA.
- HODGKIN, A. L. & HUXLEY, A. F. (1952). A quantitative description of membrane current and its application to conduction and excitation in nerve. *Journal of Physiology* **117**, 500–544.
- HODGKIN, A. L. & KATZ, B. (1949). The effect of sodium ions on the electrical activity of the giant axon of the squid. *Journal of Physiology* **108**, 37–77.
- HORN, R. & LANGE, K. (1983). Estimating kinetic constants from single channel data. *Biophysical Journal* **43**, 207–223.
- HUGHES, D., MCBURNEY, R. N., SMITH, S. M. & ZOREC, R. (1987). Caesium ions activate chloride channels in rat cultured spinal cord neurones. *Journal of Physiology* **392**, 231–251.
- KAY, A. R. & WONG, R. K. S. (1986). Isolation of neurons suitable for patch-clamping from adult mammalian central nervous systems. *Journal of Neuroscience Methods* **16**, 227–238.
- MCMANUS, O. B., BLATZ, A. L. & MAGLEBY, K. L. (1987). Sampling, log binning, fitting, and plotting durations of open and shut intervals from single channels and the effects of noise. *Pflügers Archiv* **410**, 520–553.
- MCMANUS, O. B. & MAGLEBY, K. L. (1988). Kinetic states and modes of single large-conductance calcium-activated potassium channels. *Journal of Physiology* **402**, 79–120.
- PATLAK, J. B., GRATTON, K. A. & USHERWOOD, P. N. R. (1979). Single glutamate-activated channels in locust muscle. *Nature* **478**, 643–645.
- RAO, C. R. (1973). *Linear Statistical Inference and its Applications*. John Wiley, New York.
- WEISS, D. S. & MAGLEBY, K. L. (1990). Voltage dependence and stability of the gating kinetics of the fast chloride channel from rat skeletal muscle. *Journal of Physiology* **426**, 145–176.